

# ASSESSMENT OF AIR QUALITY NEAR OAKLANDS ROAD

---

## SUMMARY

---

Presented below is a report evaluating the air quality at Oaklands Road, Brent as part of an urban improvement project. Concentrations of nitrogen dioxide (NO<sub>2</sub>), ozone (O<sub>3</sub>) and particulate matter (PM<sub>2.5</sub> & PM<sub>10</sub>) were continuously monitored by air quality sensors (AirNodes) at two specified locations: Oaklands Road and Cricklewood Broadway. Construction work was carried out partway through this period to pedestrianise the end of Oaklands Road and prevent access by traffic, with an end goal of reducing the air pollution levels by 5%.

The most notable results of the monitoring period are as follows:

- 20% reduction in NO<sub>2</sub> from local sources at Oaklands Road (from 32% to 12%)
- 13% reduction in O<sub>3</sub> from local sources at Oaklands Road (from 50% to 37%)
- Decrease in average NO<sub>2</sub> at Oaklands Road by 2.6 ug/m<sup>3</sup>
- Clear peaks in NO<sub>2</sub> concentrations occurred at 09:00 and 18:00 at Oaklands Road
- Continuously elevated levels of NO<sub>2</sub> from 09:00 till 18:00 at Cricklewood Broadway
- Concentrations of PM<sub>2.5</sub> & PM<sub>10</sub> were generally on the threshold of the annual mean exposure limit suggested by the World Health Organisation (WHO)

Traffic and footfall levels were greatly impacted by the COVID-19 pandemic and the full impact of the project can be more accurately depicted when these variables return to normal. However, given that the local contribution of most pollutants has been reduced, a general improvement in air quality is expected. In addition, further steps to improve traffic management on Cricklewood Broadway would also be beneficial. Preventing vehicles from idling by maintaining a steady flow of traffic would reduce emissions associated with mechanical processes in the brake system, engine or between the tyre-road interface.

To summarise, the project was successful in meeting the targeted reduction in pollutants and increasing the awareness of the specific environmental context in the area under consideration.

---

## INTRODUCTION

---

Road traffic is a major source of air pollution that harms human health and the environment [1]. Vehicles emit a range of pollutants including nitrogen oxides ( $\text{NO}_x$ ) and particulate matter (PM). The EU and WHO has set limit values for the maximum amount of air pollution citizens should breathe but urban populations are still exposed to levels of  $\text{NO}_x$  and PM above these limits, mainly due to passenger cars and vans circulating in these areas [2, 3].  $\text{NO}_x$  is a mixture of nitric oxide (NO) and nitrogen dioxide ( $\text{NO}_2$ ), where  $\text{NO}_2$  is a toxic gas. In the air, NO is also converted to  $\text{NO}_2$  in a process that forms ozone ( $\text{O}_3$ ). In addition,  $\text{NO}_x$  emissions also form secondary particles and contribute to acidification and eutrophication, resulting in damage to ecosystems. Predominantly  $\text{NO}_2$  is considered a secondary pollutant, which is formed in the atmosphere by the reaction of NO with  $\text{O}_3$ ; however,  $\text{NO}_2$  is also emitted as a primary pollutant, which is directly emitted into the atmosphere by combustion processes. On roadside locations,  $\text{NO}_x$  is predominantly in the form of NO, whereas in areas away from combustions sources  $\text{NO}_x$  predominantly exists in the form of  $\text{NO}_2$  due to the conversion of NO into  $\text{NO}_2$  in the atmosphere.

To better understand the depth of the problem, the detection of the pollutants of interest is necessary. Traditionally, conventional air pollution monitoring is based on static measurement stations with high-precision instruments. However, these stations have high initial investment, production and maintenance costs, which limits their deployment density [4, 5]. This yields high-quality data for the areas around the monitoring station, but the spatial and temporal resolution is limited [6]. Therefore, there has been a great interest in the potential of sensors having lower cost, commonly referred to as *low-cost sensors*, which often is more than an order of magnitude less than the corresponding high-quality air monitoring instrument [7, 8]. In the last decades, the development of low-cost sensors has evolved rapidly due to technological progress and the development of wireless communication systems. Low-cost sensors have a small size and low production cost and provide data of high time resolution. Even though the technologies still evolve and enhance, the already available low-cost sensors represent a novel alternative or supplement to the sparse conventional air monitoring stations, which provide useful insights into the patterns and sources of air pollution.

Two low-cost sensors have been deployed by AirLabs in Cricklewood, London, UK, at Oaklands Road and Cricklewood Broadway, to investigate the air quality near those streets. Cricklewood Broadway is characterised by high traffic volumes and congested traffic and as such is considered to be the primary source of pollution in the area. However, it should be noted that many factors can contribute to air pollution, including (i) the pollution from local traffic, (ii) the background pollution that enters the road, (iii) formation of pollution and (iv) road's geometry and physical characteristics. The road's physical characteristics are important



is quite rare. Other weather stations in the region show similar characteristics, and it is expected that this provides an accurate representation of the ambient winds experienced at the Oaklands Road site.

Assuming the primary local source of pollution is from vehicles on Cricklewood Broadway, the CFD simulations showed that (1) for typical wind conditions (i.e., ambient winds from the southwest and southeast), the airflow dynamics are orientated such that minimal pollution is transported into the area, (2) for ambient winds from the northwest and northeast, low concentrations of pollution may be transported into the area; however, winds from these directions are rather uncommon. It should be noted that the CFD simulations represent idealised situations that cannot incorporate the full complexity of the situation. Nevertheless, it is expected that these results capture the essential characteristics of the airflow and pollutant distributions that are likely to be observed at the site.

The main goal of this report is to describe and assess the air quality at these streets and compare the air quality pre and post pedestrianising. The goals of this air quality monitoring are (1) to provide the local community and users of the zone with visible information on the air quality both within the pedestrian zone and on Cricklewood Broadway, (2) to provide the London Borough of Brent, as well as the local community, information regarding the impacts on air quality achieved through the project and (3) to provide observational validation of the results suggested by the modelling study.

In the following sections, details of the different sensing mechanisms of the applied low-cost sensors are described. Subsequently, the results of the air quality assessment before and after the construction work are presented, whilst the last section provides a summary of the results and overall recommendations arising from the study. Within this report, the main focus will lie on NO<sub>2</sub> since this pollutant is emitted directly from traffic and therefore would be directly affected by pedestrianising.

## LOW-COST SENSORS

---

Two types of low-cost sensors are used in this project. At AirLabs, these sensors are assembled in weatherproof plastic housings with full exposure to ambient air (referred to as the *AirNode*). The housings contain inlets for the low-cost sensors and openings for ventilation. The main parts of the AirNodes are the low-cost sensors, fans and electronic components. The fans ensure that the air is actively and steadily sampled into the AirNode. The electronics primarily consist of printed circuits boards (PCBs) with micro-controllers and connection cables. Each AirNode is powered by a USB cable for operation, signal processing and data upload. The AirNodes create a wireless local network. Using this network, the AirNodes can be configured to connect with another WIFI network, which is used to transmit the raw data to AirLabs' AirIntel cloud-based data management platform. The deployed AirNodes include low-cost sensors for measuring NO<sub>2</sub> and O<sub>3</sub> (Metal oxide gas sensor: MiCS-6814 from SGX Sensortech) as well as PM<sub>2.5</sub> and PM<sub>10</sub> (Optical particle counter: SDS-011 from Nova Fitness Co., Ltd.), at a 1-minute time resolution. The AirNodes are mounted on and powered by lamp posts, approximately two and a half to three meters above street levels along the roads. This height ensures that the devices remain out of reach of the general public. Before deployment, the AirNodes were calibrated in the laboratory.

### METAL OXIDE SENSOR

Metal oxide sensors' (MOS) working principle is based on the change in its resistance or conductivity due to various reactions between gases in the surrounding atmosphere and sensor surface. Among many techniques, semiconducting sensing, a simple and inexpensive method for monitoring gases, offers high sensitivity and selectivity. Their sensing mechanism is based on the change of the electrical conductivity due to exposure to reducing or oxidizing gases. In the air, this phenomenon causes the MOS sensors to exchange electrons with the target gas at a certain rate, thereby affecting the sensor's resistance, yielding a signal.

### OPTICAL SENSOR

The SDS-011 sensor is an optical sensor for PM measurements. These sensors are based on light scattering properties of the particles. To measure the concentration of particles, a fan draws air into the sensors' gas cell to ensure a continuous flow of air through the sensor chamber. After entering the sensor, the air crosses the sensing area, where a laser beam illuminates the sensing chamber. When the laser induced-light strikes the particles, they scatter light in all directions. The 90° scattered light is detected by a photodiode detector leading to a time-dependent intensity curve. The sensor also includes a light-trap in the back of the exposure chamber to avoid additional scattering of light. Subsequently, a microprocessor converts the intensity of the scattered light into particle size or mass concentrations. The sensor has a resolution of 0.3 µg m<sup>-3</sup>.

---

## DATA COLLECTION

---

The pollutants were continuously measured at the two different sites from the 12<sup>th</sup> of February 2020 until the 12<sup>th</sup> of February 2021. At the beginning of September, construction work started to pedestrianise Oakland Road. The data from the 12<sup>th</sup> of February 2020 until the 1<sup>st</sup> of September 2020 was collected (total 202 days of measurements) to assess the air quality of the period before pedestrianising. At the end of November, Oaklands Road was fully pedestrianised. Thus, data from the 1<sup>st</sup> of December 2020 until the 12<sup>th</sup> of February 2021 (73 days of measurements) was analysed to assess the air quality. Unfortunately, during the construction work, AirNodeLC217 required maintenance and had to be replaced. The replacement sensor node is called AirNode4P07.

The aim was to analyse whether pedestrianisation affected air quality. All time series were screened for outliers mainly to remove high peaks due to sensor errors. Hence each data point,  $X_i$ , for which either equation 1 or equation 2 applies, was removed

$$X_i < \bar{X} - (5 \times \sigma) \quad (1)$$

$$X_i > \bar{X} + (5 \times \sigma) \quad (2)$$

where  $\bar{X}$  is the mean and  $\sigma$  is the standard deviation of the data set. There were a few weeks of missing data, but the overall pattern of the air quality is clear.

---

## RESULTS AND DISCUSSIONS

---

In general, the variation of an air pollutant by time and day of the week can reveal useful information concerning its likely sources. Road vehicle emissions tend to follow regular patterns both on a daily and weekly basis. By contrast, some industrial emissions or pollutants from natural sources (e.g. sea salt aerosol) may have quite different patterns. Temporal variations of NO<sub>2</sub> during different hours of the week from 12<sup>st</sup> of February until the 1<sup>st</sup> of September 2020 are shown in **Figure 2**. NO<sub>2</sub> levels at both sites vary during the different time periods, however, average NO<sub>2</sub> levels are slightly greater at Cricklewood Broadway, which is expected as Cricklewood Broadway is a busier road. Generally, the variations between the two AirNodes are due to the differences in traffic density and street geometry. In **Figure 2** (top panel), the weekly cycle of NO<sub>2</sub> is shown, and the different temporal trends in concentration are seen, including the diurnal variation. The daily variations in NO<sub>2</sub> concentrations are based on the daily changes in nearby traffic and photochemical processes that lead to a difference between day and nighttime concentrations of NO<sub>2</sub>. There is a prominent increase in concentrations during the morning rush hours on weekdays as compared to the weekend. It is clearly shown that NO<sub>2</sub> levels are greater at Cricklewood Broadway than at Oaklands Road. **Figure 2** (bottom panel, right) shows the variation over days of the week, and there is a

significant variation between the two sites on various days. The highest NO<sub>2</sub> levels are shown on Wednesdays at both monitoring sites, whereas the lowest levels are seen on the weekends. There is a more significant difference between NO<sub>2</sub> levels on weekdays compared to the weekend at Cricklewood Broadway than at Oaklands Road. This again indicates that traffic is the major source of NO<sub>2</sub> on Cricklewood Broadway.

As seen in **Table 1**, higher concentrations of particulate matter are seen at Oaklands Road compared to Cricklewood Broadway. Particulate matter in the size-fractions measured within this study is not a direct proxy for traffic as compared to for instance NO<sub>2</sub>. Particles originating from traffic exhaust are mainly in the ultrafine region. However, traffic can contribute to mechanically formed particles, which originates from re-suspended dust, wear of road surface materials and tyres as well as from the usage of brakes. Long-range transport is often the major source of PM<sub>2.5</sub> and PM<sub>10</sub> in urban areas. Even though the major contributor of O<sub>3</sub> is regional sources, it is still affected directly by traffic, since O<sub>3</sub> and NO<sub>2</sub> are closely correlated in their photochemistry. High concentrations of O<sub>3</sub> near a busy road is limited since O<sub>3</sub> rapidly reacts with traffic-induced NO and forms NO<sub>2</sub>.

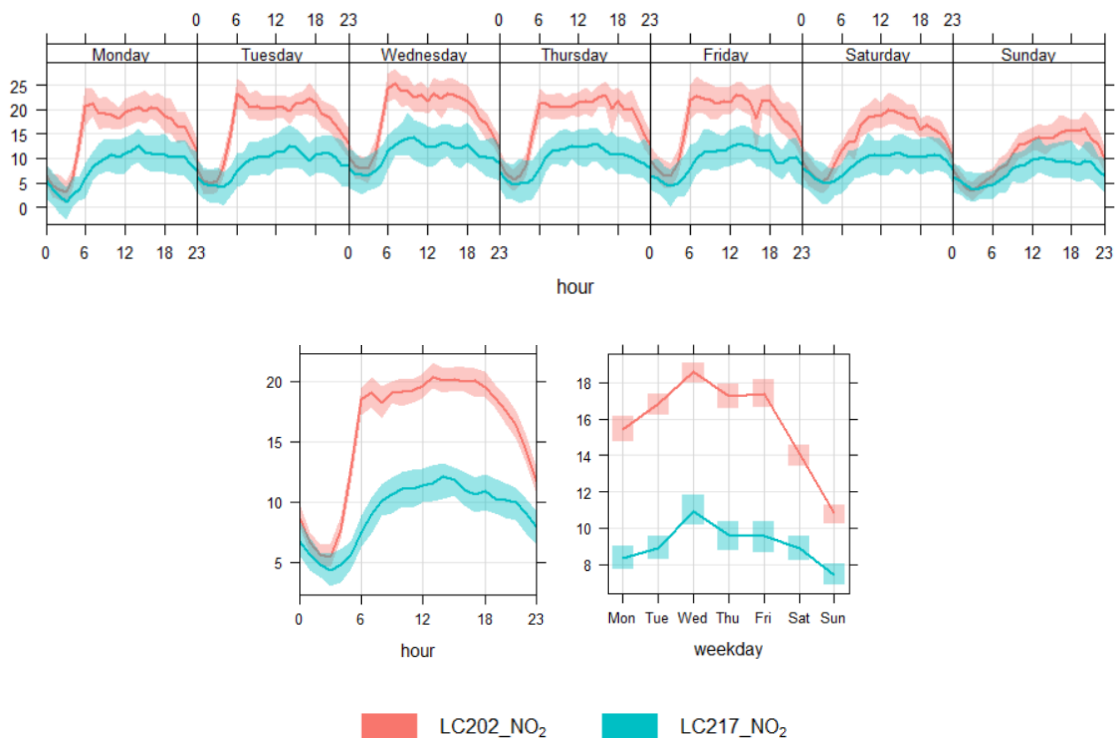


**Figure 2:** Time variation of NO<sub>2</sub> (µg m<sup>-3</sup>) measured by AirNodeLC202 (red) and AirNodeLC217 (blue) before pedestrianisation. Illustrated as mean and 95% confidence interval in the mean. Weekly variation (top), weekly variation (bottom, left) and hourly variation (bottom, right). Note the different scaled axes.

**Table 1:** Average for NO<sub>2</sub>, O<sub>3</sub>, PM<sub>2.5</sub> and PM<sub>10</sub> measured by LC202, LC207 and P07 averaged over the period before the construction work (Pre) and after the construction work (Post).

Sensor	NO <sub>2</sub>		O <sub>3</sub>		PM <sub>2.5</sub>		PM <sub>10</sub>	
	Pre	Post	Pre	Post	Pre	Post	Pre	Post
LC202	15.8	16.5	36.1	51.3	6.8	8.7	14.4	17.6
LC217/P07	13.6	11.0	42.6	56.0	9.1	12.0	30.6	22.0

After November, Oaklands Road was fully pedestrianised. Thus, data from the 1<sup>st</sup> of December 2020 until the 28<sup>th</sup> of February 2021 is analysed to assess whether pedestrianising affected the air quality. The temporal variation of NO<sub>2</sub> during different hours of the week measured by AirNodeLC202 and AirNode4P07 is shown in **Figure 2** and key numbers are highlighted in **Table 1**. There is more variation between the NO<sub>2</sub> levels obtained by the two sensors over time of the day and day of the week, as compared to the temporal variations seen before the construction work period. This is seen from the 95% confidence interval. However, the same trend is clear, with a slightly higher NO<sub>2</sub> concentration at Cricklewood Broadway compared to Oaklands Road. This variation can be due to ‘abnormal’ weekly changes in traffic density over a day or changing meteorological conditions. It should be noted that the period after the pedestrianisation only includes 36.5% of the total amount of data used for the period before the pedestrianisation. Thus, the variation seen in the data may originate from the relatively small amount of data. The weekly cycle of NO<sub>2</sub> is shown in **Figure 2** (top panel) together with the different temporal trends in concentration. There is a prominent increase in concentration during the morning rush hours on weekdays as compared to the weekend at both sites.

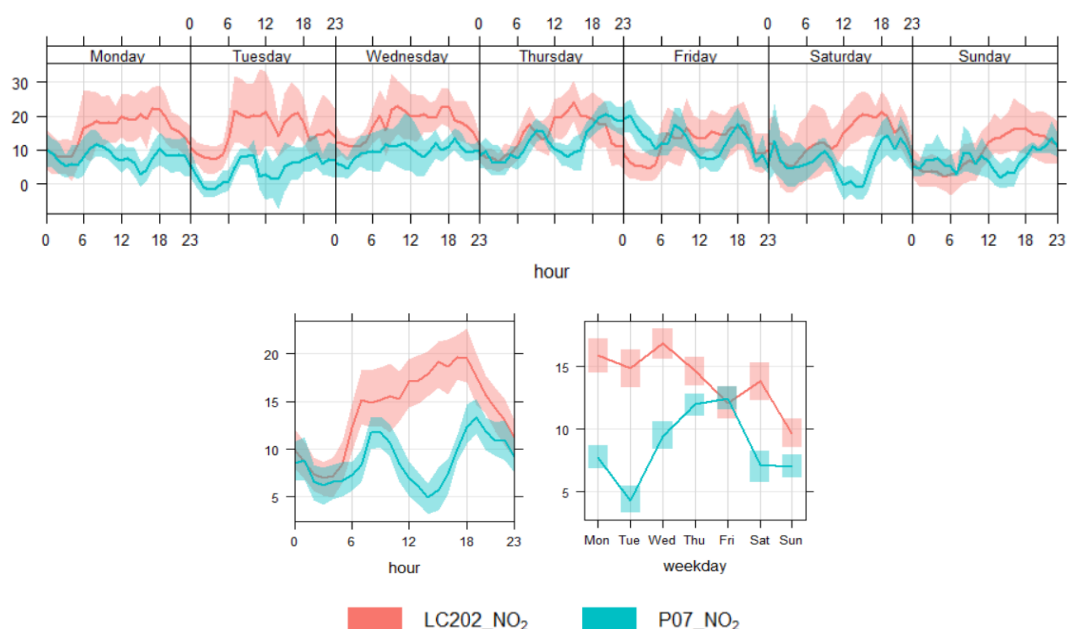


**Figure 2:** Time variation of NO<sub>2</sub> (µg m<sup>-3</sup>) measured by AirNodeLC202 (red) and AirNode4P07 (blue) after pedestrianisation. Illustrated as mean and 95% confidence interval in the mean. Weekly variation (top), weekly variation (bottom, left) and hourly variation (bottom, right). Note the different scaled axes.

The increase is generally smaller for AirNode4P07 at Oaklands Road, and since the road is pedestrianised, the pollution originates from sources further away and probably from Cricklewood Broadway.

**Figure 2** (bottom-panel, left) displays the average variation over a day and there is a slight variation between the two different sensor nodes. The NO<sub>2</sub> level obtained by AirNodeLC202 increases rapidly during the morning rush hours and keep rising steadily during the day, where it, at 18:00 starts to decrease again. AirNode4P07 displays the bimodal diurnal distribution of NO<sub>2</sub> during the day, with the two peaks around 09:00 and 18:00 reflecting the morning and evening rush hours. There is also more variation in **Figure 2** (bottom-panel, right) between the two sites. For AirNodeLC202, the highest NO<sub>2</sub> concentrations are still seen on Wednesdays, where for AirNode4P07 highest concentration is seen on Fridays. However, both sensors agree that weekends yield the lowest concentrations of NO<sub>2</sub>.

The variation within each site can be explained by meteorology and differences in traffic patterns. In general, the evening peaks of NO<sub>2</sub> is more pronounced in autumn and winter as compared to spring/summer differences, which can be attributed to seasonal boundary layer height conditions and subsequent lower median wind speeds, and a change in the diurnal wind pattern by season. As the height of the boundary layer increases in spring and summer, wind speed increases at a faster rate throughout the day, increasing dispersion. There are differences in traffic patterns over the study period due to the Covid-19 pandemic. During lockdowns, high reductions in traffic have seen observed, and in general, more people work from home multiple days during the week, which affects the bimodal diurnal distribution of NO<sub>2</sub> during the day.

## SPECTRAL ANALYSIS

Time series of hourly air quality data contain meaningful information when analysed deeper. Typical air quality time series exhibit hourly, daily, weekly, seasonal, yearly, and other periodic behaviours, which if identified could help to predict the time series variables and reveal the source of the pollutants. These hidden periodicities are caused by fluctuations of meteorological conditions, the Earth's daily rotation, seasonal fluctuations in solar radiation, and human activities. The most common tool for analysing the periodicities is the Fourier Transform (FT), and it has been extensively used for decades. However, it does not perform as well when dealing with air quality data, because of the unevenly spaced time points over time due to technical and practical problems during the monitoring. This unevenly spaced or missing data can be overcome by using methods such as the discrete Fourier transform (DFT) with mean-gapping. This method is evaluated by applying the fast Fourier transform (FFT) algorithm after filling the gaps and missing values with the mean.

There is a strong relation between temporal and spatial scales of air pollutants. In this context, short-term fluctuations of the pollutant concentrations are related to local-scale phenomena, including local dispersion conditions, local emissions and short-term atmospheric

chemistry. On the contrary, seasonal changes in the emissions and long-range transport of the pollution will contribute to the spectrum at low frequencies. The recorded air quality data was used for the spectral analysis after removing the linear trend by subtracting the average concentration obtained by each sensor. The contributions of local and regional sources to the pollutants are calculated based on the determined amplitudes and frequencies of each pollutant. The local sources are revealed in the high-frequency periodogram ( $> 0.0139 \text{ h}^{-1}$ ), whereas the regional sources are revealed in the low-frequency periodogram ( $< 0.0139 \text{ h}^{-1}$ ).

**Figure 3** displays the periodograms of  $\text{NO}_2$  from AirNodeLC202 and AirNodeLC217, respectively. The periodogram of  $\text{NO}_2$  for AirNodeLC202 features three distinct peaks in the high-frequency region at  $0.021 \text{ h}^{-1}$  (48 h),  $0.041 \text{ h}^{-1}$  (24 h) and  $0.062 \text{ h}^{-1}$  (16 h). In addition, one peak is identifiable at  $0.084 \text{ h}^{-1}$  (12 h). The periodogram of  $\text{NO}_2$  from AirNodeLC217 also reveals two distinct peaks in the high-frequency area at  $0.021 \text{ h}^{-1}$  (48 h),  $0.041 \text{ h}^{-1}$  (24 h). These two peaks at 24 and 48 hours are mainly originating from the diurnal variation of  $\text{NO}_2$  over a day. The peaks at 16 and 12 hours can be related to the daily traffic cycles or daily meteorological changes. For both sensors, a few peaks are located in the low-frequency region, which originates from changes over either synoptic- or larger scale.

**Table 2** lists the calculated percentages of local and regional contributions. AirNodeLC202 yields the highest percentages of the local contribution across all pollutants. This AirNode is located at Cricklewood Broadway, where there is increased traffic. The most important source of  $\text{NO}_2$  is traffic, the results suggest that the majority of the source is regional, which could originate from long-range transport.  $\text{O}_3$  is a secondary pollutant, meaning that there are no direct emission sources. It can, however, be created but also converted from emissions of  $\text{NO}_x$ . Generally,  $\text{PM}_{10}$  like  $\text{PM}_{2.5}$  can be transported through the air, but not as far as  $\text{PM}_{2.5}$ . However, especially, in the cities and near busy roads, there is a contribution to  $\text{PM}_{10}$  from local traffic due to whirling by the movement of vehicles, and they are formed in the mechanical processes in the tyre-road interface and brakes and engine. A bus stop is located in front of the sites, which possibly is a major contributor to the locally sourced particulate matter.

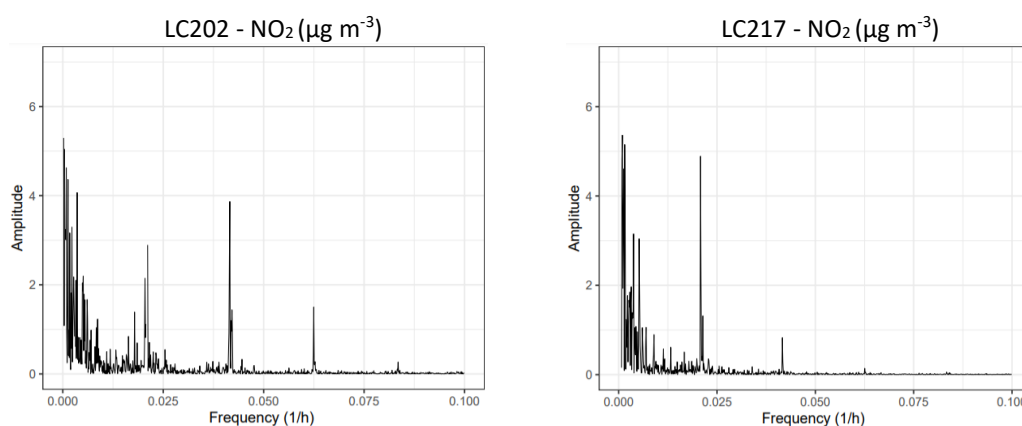


**Figure 3:** Periodograms for  $\text{NO}_2$  ( $\mu\text{g m}^{-3}$ ) by AirNodeLC202 and AirNodeLC217. Note the different scaled axes. Only a certain frequency window is shown for the sake of clarity.

**Table 2:** Local and regional contribution of NO<sub>2</sub>, O<sub>3</sub>, PM<sub>2.5</sub> and PM<sub>10</sub> given in percentage for AirNodeLC202, AirNodeLC217 and AirNode4P07 during the pre- and post construction period.

Sensor	NO <sub>2</sub>		O <sub>3</sub>		PM <sub>2.5</sub>		PM <sub>10</sub>	
	Regional	Local	Regional	Local	Regional	Local	Regional	Local
<b>Pre construction work</b>								
LC202	55	45	46	54	51	49	55	45
LC217	68	32	50	50	60	40	59	41
<b>Post construction work</b>								
LC202	65	35	59	41	67	33	60	40
P07	88	12	64	37	62	38	54	45

The periodograms of NO<sub>2</sub> from AirNodeLC202 and AirNodeP07 after the pedestrianisation are shown in **Figure 4**. The periodogram of NO<sub>2</sub> for AirNodeLC202 shows two close peaks in the high-frequency region around 0.025 h<sup>-1</sup> (48 h). The additional significant peaks are located in the low-frequency region. The same trend is seen in the periodogram of NO<sub>2</sub> for AirNodeP07, where most of the dominant peaks are in the low-frequency area and a single significant peak is seen in the periodogram of NO<sub>2</sub> for AirNodeP07 at 0.041 h<sup>-1</sup> (24 h). Based on **Table 2**, the local contribution or daily variation slightly differ from the period before the pedestrianisation. The local contribution of NO<sub>2</sub> accounts for 35 and 12% for AirNodeLC202 and AirNodeP07, respectively. Thus, there is in general a smaller contribution from local sources as compared to the period before the pedestrianisation where the local contribution was 45 and 32%, respectively. This decrease is likely to originate from the pedestrianisation of Oaklands Road. The pedestrianisation also affected the air quality at Cricklewood Broadway, since less traffic of a specific type would pass the area. Before the pedestrianisation, when vehicles were driving towards Cricklewood Broadway, they would slow down to get to Cricklewood Broadway. Frequent stop, acceleration and idling are the driving styles, which emit most NO<sub>2</sub> depending on the type and age of the respective vehicle.

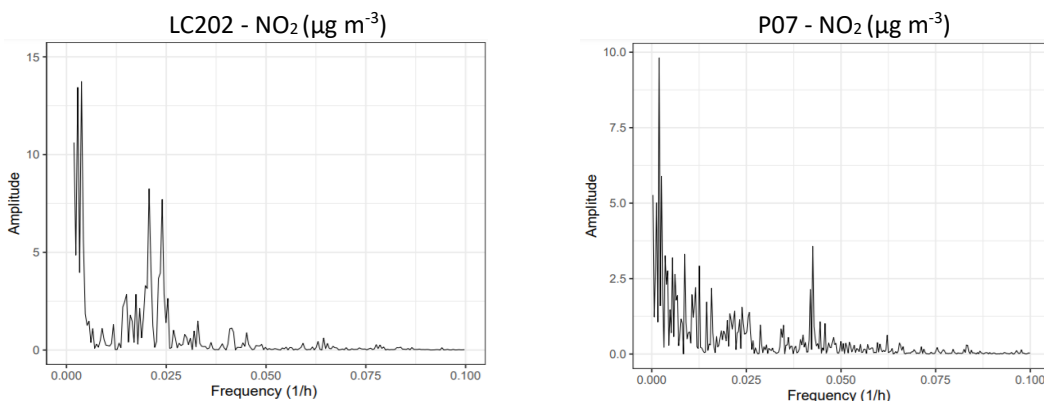


**Figure 4:** Periodograms for NO<sub>2</sub> (µg m<sup>-3</sup>) by AirNodeLC202 and AirNodeLC202. Note the different scaled axes. Only a certain frequency window is shown for the sake of clarity. Note the different scaled axes.

## BIVARIATE POLAR PLOTS

A key component of air pollution is to determine how variables are related to each other. Exploring the relationships between the different pollutants and meteorological parameters can be particularly useful. It is because pollutants with high levels of correlation often originate from the same source or have a similar physical or chemical transformation in the atmosphere [9, 10]. Wind speed and direction have been shown to provide essential information, typically, leading to the suggestion of source location [11, 12]. A powerful tool for this source characterization is bivariate polar plots, which is a way to visualize mean pollutant concentrations calculated for wind speed and wind direction bins. The wind direction is displayed from 0 to 360° clockwise on the angular axis, whereas wind speed is shown on the radial scale.

The bivariate polar plots are shown in **Figure 5**. For AirNodeLC217, the highest NO<sub>2</sub> concentrations are obtained with winds from the southwest and northeast as well as when the wind speed is low. These higher NO<sub>2</sub> values can be associated with the orientation of the road. The lowest values of NO<sub>2</sub> are seen at the higher wind speeds from the northwest and southeast. The bivariate polar plots for O<sub>3</sub> (seen in Appendix), generally show the opposite result than the bivariate polar plots for NO<sub>2</sub>, with the highest values from northwest and southeast. In addition to NO<sub>2</sub>, NO can also be emitted from traffic. During sunny days, NO<sub>2</sub> photolyses and the product subsequently form O<sub>3</sub>. However, at a busy road with NO emissions, O<sub>3</sub> rapidly reforms to NO<sub>2</sub>. Thus, high O<sub>3</sub> concentrations are limited on a busy road.

The CFD simulations showed that for ambient winds from the southwest and southeast the airflow dynamics are orientated such that minimal NO<sub>2</sub> pollution is transported into the area. This calculation was performed under the assumption that the primary source of pollution is from vehicles on Cricklewood Broadway, thus these results show the pollution sources located at Oaklands Road. As also written in the modelling report, the associated NO<sub>2</sub> concentration from the southeast is transported along the axis of the pollution source. Consequently, the NO<sub>2</sub> concentration is confined primarily to the main road. Further, since the airflow along Oaklands Road is directed towards the main road, the NO<sub>2</sub> concentration at the site is low.

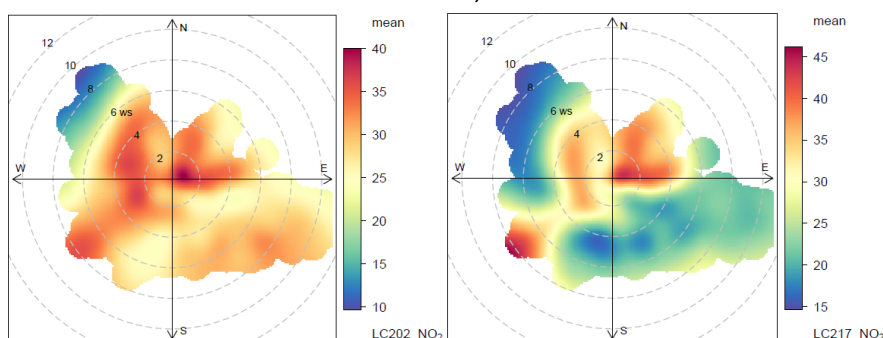


**Figure 5:** Bivariate polar plots of NO<sub>2</sub> for hourly average data for AirNodeLC202 (left) and AirNodeLC217 (right). The colour scale shows the concentrations and the radial scale shows the wind speed, which increases from the centre of the plot radially outwards. Note the different scaled axes.

## REFERENCE STATIONS

The AirNodes were compared with data obtained by air quality monitoring stations. This comparison allows assessment of the local and regional component of the pollution data as well as check whether the baselines follow the same tendencies. Peaks in the times series that are not shown by the reference instruments may be attributable to the local sources. These peaks for the time series of O<sub>3</sub> cannot be directly associated with the local sources, however, since O<sub>3</sub> is a secondary pollutant formed via reactions with primary pollutants (e.g. NO or volatile organic compounds (VOCs)). If a pattern is clear across the references and the AirNodes, it can be attributed to changes on larger scales. **Figure 6** displays the correlation matrix of all the reference stations nearby and the AirNodes. There are in general poor correlations between the AirNodes and the references with the highest r<sup>2</sup>-value being 0.20. The lack of correlation was expected since the AirNodes are located relatively far from the references. It should be noted that the highest r<sup>2</sup>-value between the reference stations is 0.66, so a value above this one, would not be expected. The correlation of determination (r<sup>2</sup>) between the two AirNodes' NO<sub>2</sub> measurements is 0.58, indicating that some of the concentration of NO<sub>2</sub> originates from the same source, i.e. emissions from traffic at Cricklewood Broadway is entering Oaklands Road.

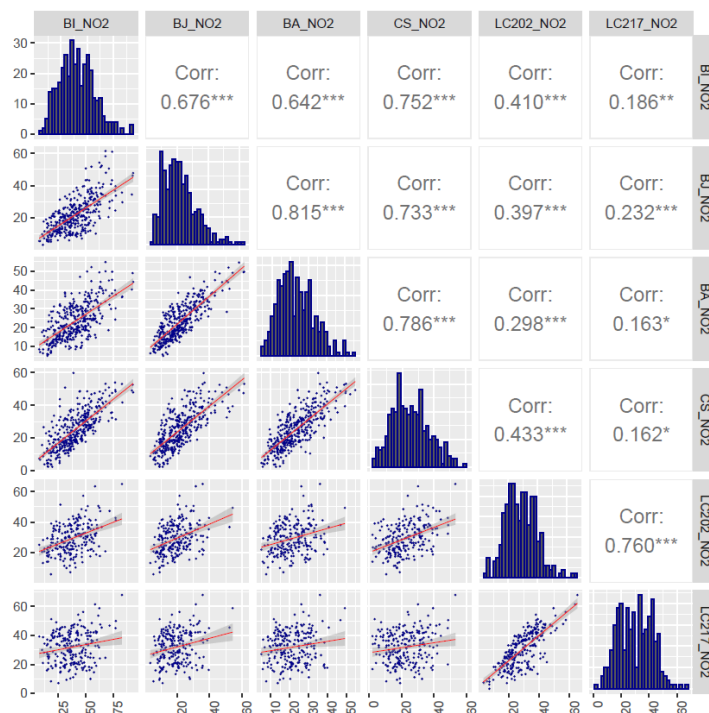


**Figure 6:** Correlation matrix showing the graphical (scatterplot and frequency distribution histogram) and statistical (Pearson correlation coefficient) pairwise correlation between four different reference stations and the AirNodes. BI = Brent - Ikea, BJ = Brent – John Keble Primary school, BA = Brent – ARK Franklin Primary Academy, CS = Camden – Swiss Cottage.

## CONSTRUCTION WORK

Construction activities tend to generate dust and can cause impacts on the air quality of surrounding areas. During the pre-construction period, the average  $PM_{2.5}$  concentration was  $9.1 \mu\text{g m}^{-3}$  at Oaklands Road, whereas under the construction work, the  $PM_{2.5}$  levels increased to  $12.8 \mu\text{g m}^{-3}$ , giving a 29% increase but this construction work, by its nature, is temporary. The World Health Organisation (WHO) has clear recommended exposure limits for certain key air pollutants, to which these ambient pollutant concentrations can be compared. According to the WHO, average exposure to  $PM_{2.5}$  over a year should be limited to  $10 \mu\text{g m}^{-3}$  [2]. The average concentration of  $PM_{2.5}$  during the construction work is higher than this exposure limit and as seen in **Figure 7**, the concentration occasionally went above the 24-hour average limit at  $25 \mu\text{g m}^{-3}$ .

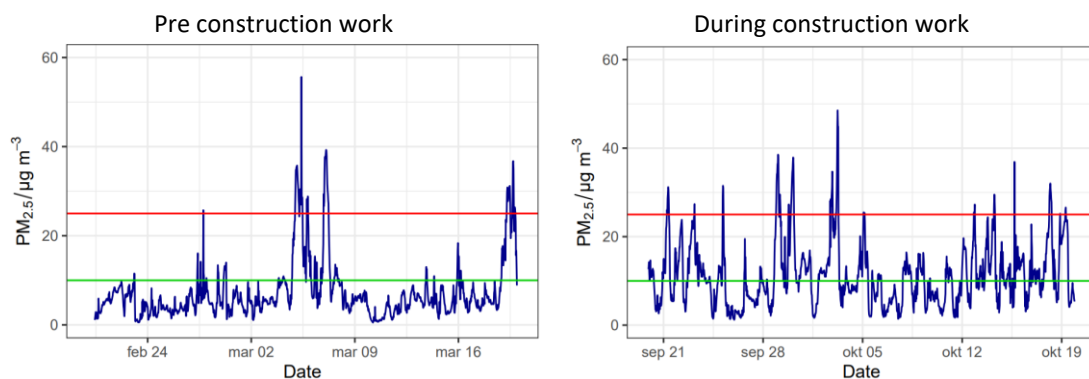


**Figure 7:** Time series of  $PM_{2.5}$  during the pre construction period (left) and the construction work period (right). World Health Organisation's yearly and 24-hour average limits marked with green and red horizontal lines, respectively. Only one-month windows are shown for clarity.

## LOCKDOWN

To fight against the spread of COVID-19, most countries in the spring of 2020 implemented different lockdown strategies, which resulted in a reduction of transportation, industry and commercial activities during the lockdown. **Figure 8** illustrates the monthly average of  $NO_2$  during 2020 at Cricklewood Broadway. During March and April, the average concentration drops rapidly, whereas it steadily increases until August, hereafter it decreases again. This variation over the year is attributed to the lockdowns and abnormal traffic characteristics.

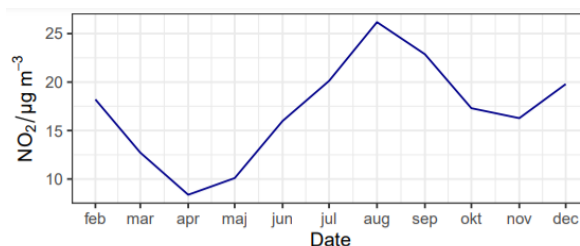


**Figure 8:** Time series of monthly averages  $NO_2$  measured at Cricklewood Broadway in 2020.

---

## CONCLUSION AND RECOMMENDATION

---

An assessment of the air quality for the area around the Oaklands Road site is presented. The analysis has been divided into the period before and the period after the pedestrianisation of Oaklands Road.

NO<sub>2</sub> value at Oaklands Road have improved to be 5.5 ug m<sup>-3</sup> lower than Cricklewood Broadway values, a difference of twice that of pre-construction levels. Despite O<sub>3</sub> levels being higher at Oaklands Road than at Cricklewood Broadway, the local contribution to this total value was lower than pre-construction (37% compared to 41%).

PM<sub>2.5</sub> & PM<sub>10</sub> concentrations remained the same or increased marginally, with similar contributions coming from local and regional sources. Both types of pollutant can be transported through the air, however PM<sub>2.5</sub> can be carried over larger distances, as shown by the regional vs local balance at both sites. Therefore, in order to have a meaningful reduction in these concentrations, a wider scale traffic management solution would be recommended to either reduce the quantity of traffic or prevent idling and maintain a continuous flow of vehicles.

The correlation between reference station data and that of the AirNodes demonstrates the importance of granularity in a sensor array. Measurements taken at reference stations provide an accurate, highly calibrated picture but only at a few locations; data in between these points has to be interpolated/modelled to compensate and therefore carries a level of uncertainty.

The COVID-19 pandemic provided an interesting insight into how traffic levels impact the air quality in areas. A dip in NO<sub>2</sub> concentrations was clearly seen for the months of March and April, before steadily rising again as lockdown restrictions were lifted towards August.

In summary, a significant amount of the NO<sub>2</sub> concentration in the area is emitted from traffic and the preliminary results find that the pedestrianisation of Oaklands Road has decreased this pollutant.

Report prepared by AirLabs, March 2021

Louise Bøge Frederickson, MSc, PhD student

Archie Waller, MSc, Product Development Project Engineer

Mark Saunders, MA (Oxon), MBA, Head of Commercial

---

## REFERENCES

---

1. T. F. Stocker, D. Qin, G. K. Plattner, M. Tignor, S. K. Allen, J. Boschung, A. Nauels, Y. Xia, V. Bex, and P. M. Midgley. IPCC: Climate Change 2013: The Physical Science Basis. Contribution of Working Group I to the Fifth Assessment Report of the Intergovernmental Panel on Climate Change. Cambridge University Press, 2013.
2. World Health Organization. *Air quality guidelines: global update 2005: particulate matter, ozone, nitrogen dioxide, and sulfur dioxide*. World Health Organization, 2006.
3. EU. EU Air Quality Directive; Technical Report Version V1; Directives; European Environmental Agency: Copenhagen, Denmark, 2008.
4. B. Maag, Z. Zhou, and L. Thiele. A survey on sensor calibration in air pollution monitoring deployments. *IEEE Internet of Things Journal*, 5:4857–4870, 2018.
5. P. Kumar, L. Morawska, C. Martani, G. Biskos, M. Neophytou, S. Di Sabatino, M. Bell, L. Norford, and R. Britter. The rise of low-cost sensing for managing air pollution in cities. *Environment international*, 75:199–205, 2015.
6. N. H. Motlagh, E. Lagerspetz, P. Nurmi, X. Li, S. Varjonen, J. Mineraud, M. Siekkinen, A. Rebeiro-Hargrave, T. Hussein, and T. Petaja. Toward massive scale air quality monitoring. *IEEE Communications Magazine*, 58(2):54–59, 2020.
7. F. Karagulian, M. Barbieri, A. Kotsev, L. Spinelle, M. Gerboles, F. Lagler, N. Redon, S. Crunaire, and A. Borowiak. Review of the performance of low-cost sensors for air quality monitoring. *Atmosphere*, 10(9):506, 2019.
8. L. Spinelle, M. Gerboles, M. G. Villani, M. Alexandre, and F. Bonavitacola. Field calibration of a cluster of low-cost available sensors for air quality monitoring. Part A: Ozone and nitrogen dioxide. *Sensors and Actuators B: Chemical*, 215:249–257, 2015.
9. D. C. Carslaw and S. D. Beevers. Characterising and understanding emission sources using bivariate polar plots and k-means clustering. *Environmental Modelling Software*, 40:325 – 329, 2013.
10. Y.-J. Liu and R. M. Harrison. Properties of coarse particles in the atmosphere of the United Kingdom. *Atmospheric Environment*, 45:3267–3276, 2011.
11. D. C. Carslaw, S. D. Beevers, K. Ropkins, and M. C. Bell. Detecting and quantifying aircraft and other on-airport contributions to ambient nitrogen oxides in the vicinity of a large international airport. *Atmospheric Environment*, 40(28):5424 – 5434, 2006.
12. E. J Westmoreland, N. Carslaw, D. C. Carslaw, A. Gillah, and E. Bates. Analysis of air quality within a street canyon using statistical and dispersion modelling techniques. *Atmospheric Environment*, 41(39):9195 – 9205, 2007.